Electronic Supplementary Material (ESI) for RSC Advances.

Fluorescent gold nanoclusters for *in vivo* target imaging of Alzheimer's disease

Lanmei Lai[a] Chunqiu Zhao[a] Xiaoqi Li[b] Xiaoli Liu[a] Hui Jiang[a] Matthias Selke[c] Xuemei Wang[a,*]

[a]State Key Laboratory of Bioelectronics, School of Biological Science and Medical Engineering, Southeast University, Nanjing 210096, China

[b]Nanjing Foreign Language School, Nanjing 210096, China

[c]Department of Chemistry and Biochemistry, California State University, Los Angeles, California 90032, United States

Supporting information

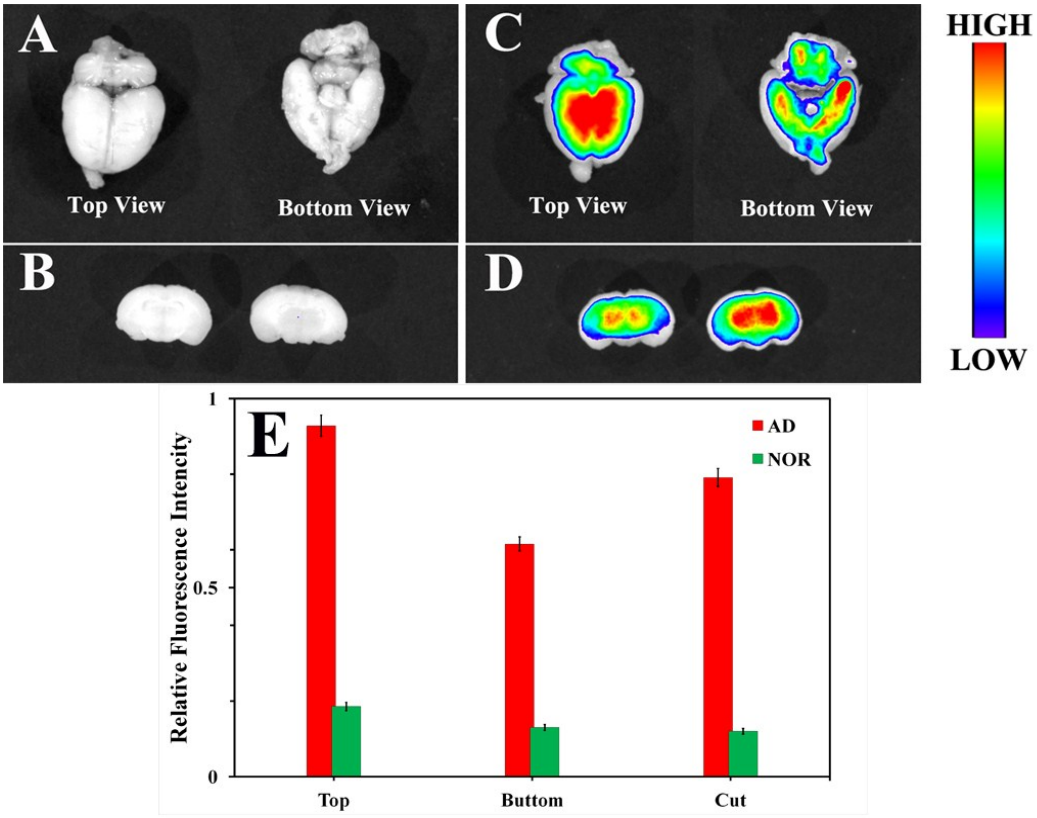

Figure S1 **(A, C)** Fluorescence imaging of the dissected brain of the normal control group of mice and Alzheimer's model mice via tail-vein injection of 10 mmol/L $HAuCl_4$ solution at 30 h post-injection. Each of the fluorescent imaging of the dissected brain was taken from two angles (top view and bottom view). **(B, D)** Fluorescence imaging of the transverse section of the normal mice's brain and AD's brain via tail-vein injection of 10 mmol/L $HAuCl_4$ solution at 30h post-injection which was cut into two parts near the hippocampus area. **(E)** The variations of mean fluorescence intensity of the cut brain **(Cut)** of the two groups.

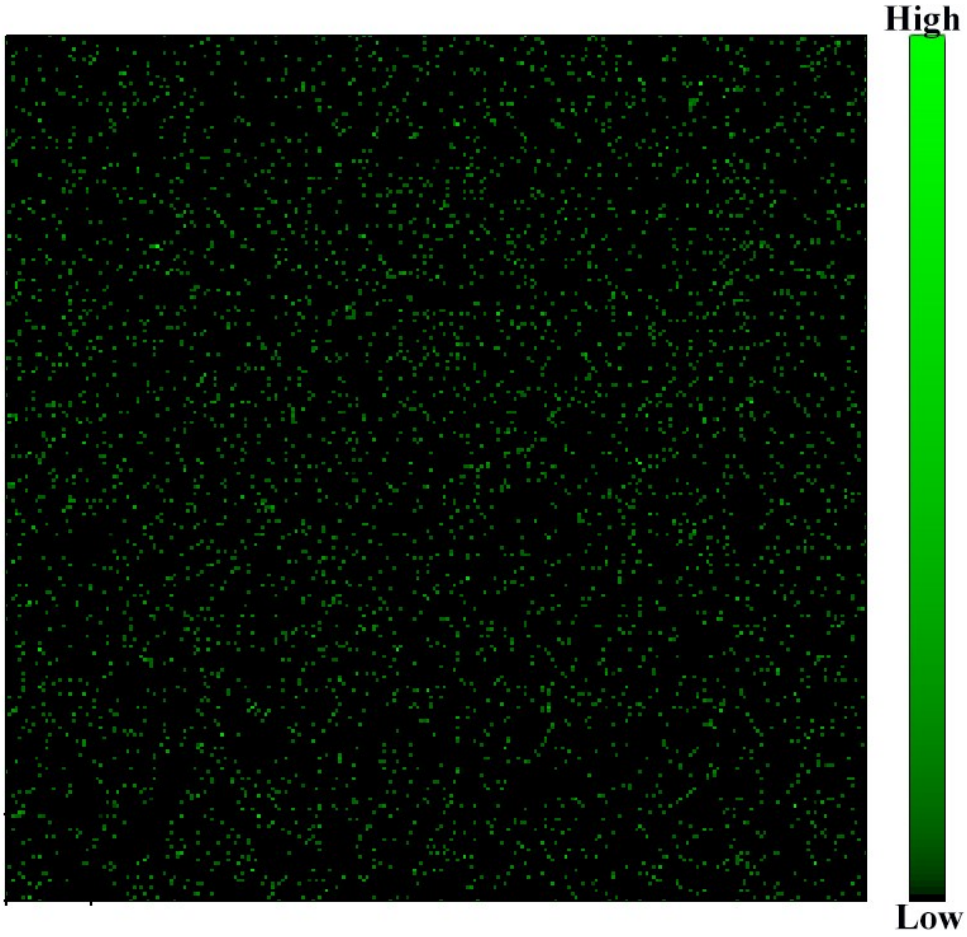

Figure S2 XPS-element mapping of the brain tissues of the AD mice via tail-vein injection of 10 mmol/L $HAuCl_4$ solution, indicating that gold nanoclusters biosynthesized specially distributed in the affected area in AD's brain.

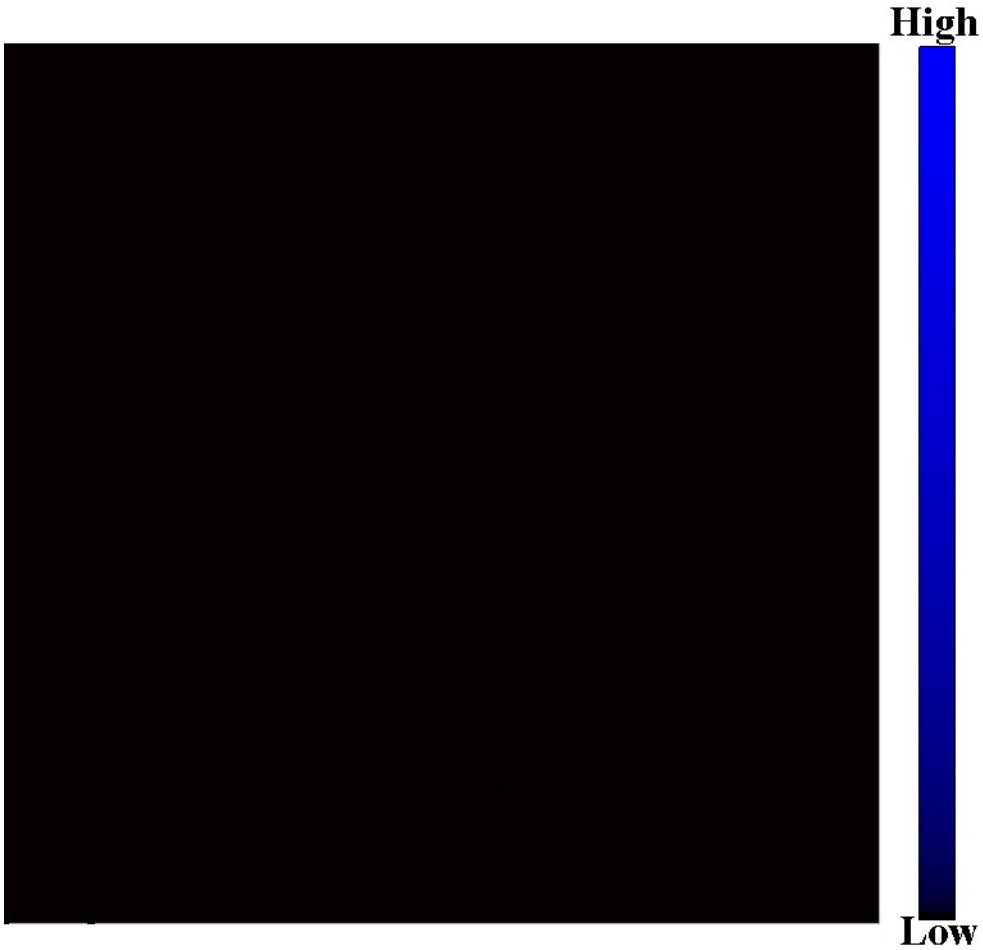

Figure S3 XPS-element mapping of the brain tissues of the blank control group of AD mice (**CON**) without injection of 10 mmol/L $HAuCl_4$ solution, indicating that there was no Au nanoclusters found in the CON's brain areas compared with that of AD's brain tissues shown in Figure S2.

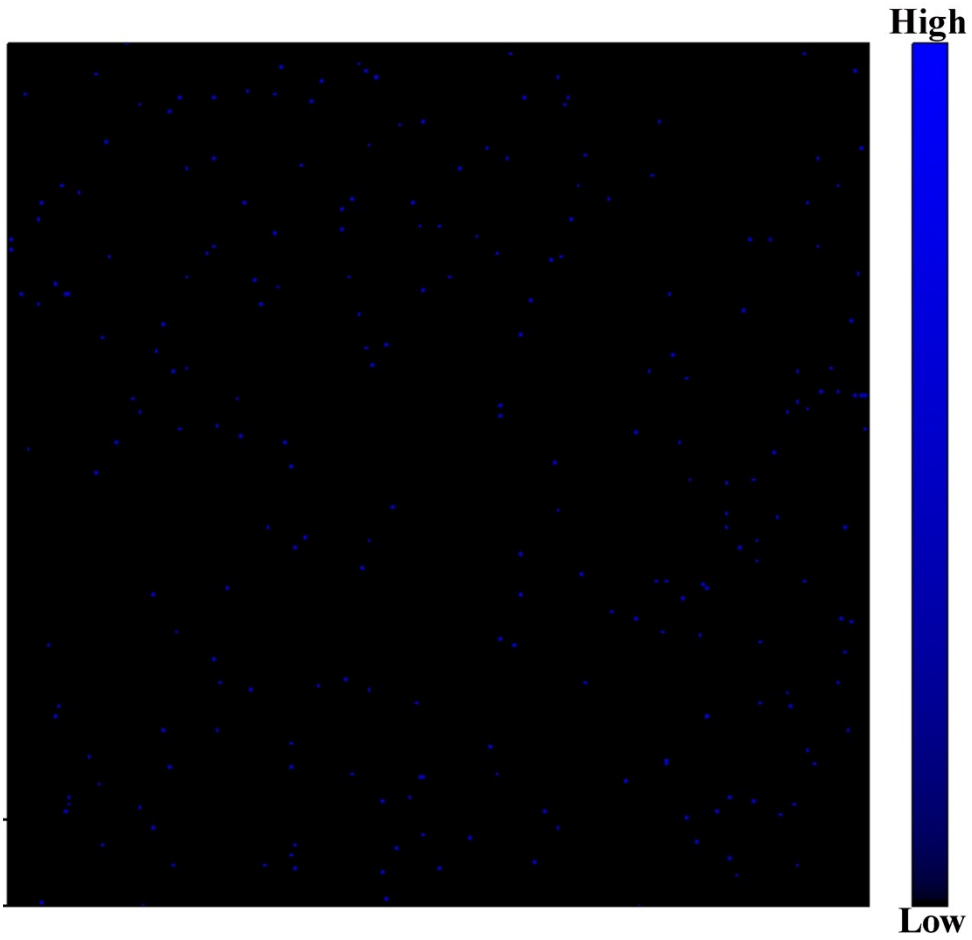

Figure S4 XPS-element mapping of the brain tissues of the normal control group of mice (**NOR**) via tail-vein injection of 10 mmol/L $HAuCl_4$ solution, with very few Au nanoclusters found in the normal brain areas compared with that of AD's brain tissues shown in Figure S2.

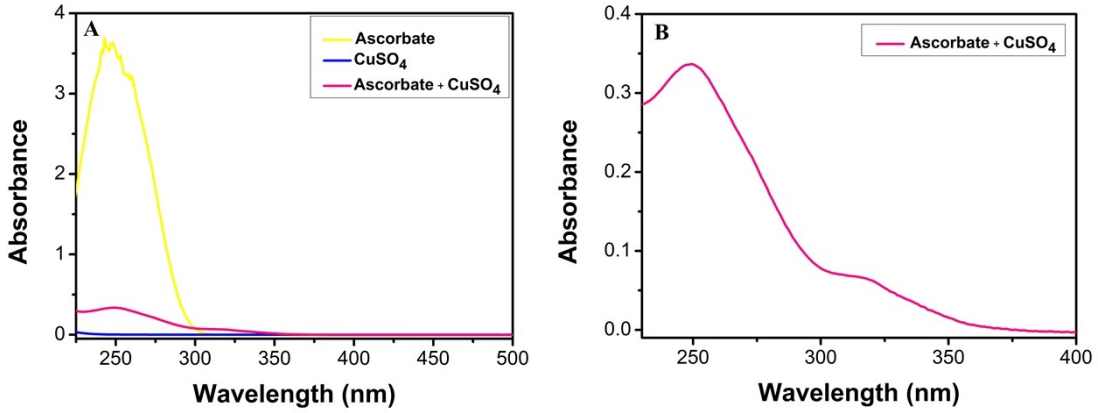

Figure S5 (**A)** UV-Vis absorption spectrum of ascorbate solution (**yellow curve**), $CuSO_4$ solution (**blue curve**) and the mixture of ascorbate solution and $CuSO_4$ solution when $CuSO_4$ solution was just added to ascorbate solution (**pink curve**) at room temperature respectively. The ultraviolet absorption peak of ascorbate solution is at 243 nm and the $CuSO_4$ solution has no ultraviolet absorption. When $CuSO_4$ solution was added to ascorbate solution, the ultraviolet absorption peak of ascorbate solution drastically decreased and there appeared a new peak at 314 nm of the complex ascorbate-Cu(II). **(B)** Enlarged UV-Vis absorption spectrum of the mixture of ascorbate solution and $CuSO_4$ solution when the $CuSO_4$ solution was just added to ascorbate solution .

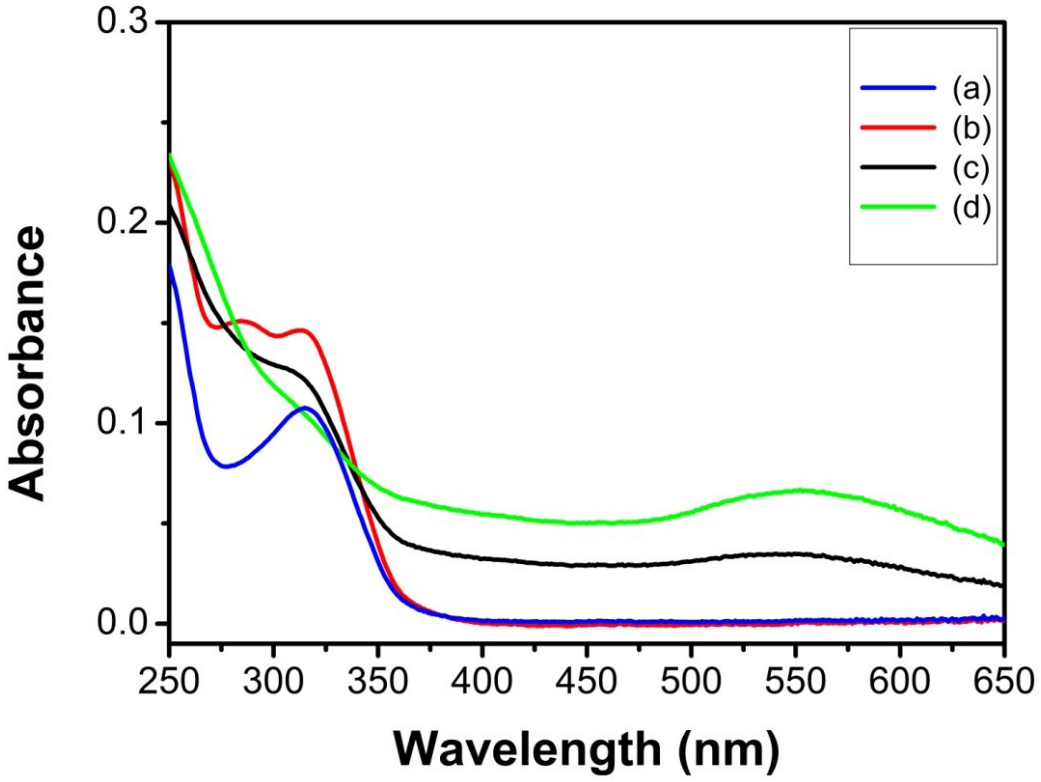

Figure S6 **(a)** UV-Vis absorption spectrum of 600 μmol/L ascorbate solution and 200 μmol/L $CuSO_4$ solution **(blue curve)** when $CuSO_4$ solution was just added to ascorbate solution for 1 minute. **(b)** UV-Vis absorption spectrum of the 600 μmol/L ascorbate solution and 200 μmol/L $CuSO_4$ solution **(red curve)** when $CuSO_4$ solution was added to ascorbate solution for about 5 minutes. **(c)** UV-Vis absorption spectrum of 600 μmol/L ascorbate solution and 200 μmol/L $CuSO_4$ solution when 10 μmol/L $HAuCl_4$ solution was added to the reaction mixture **(black curve)**. **(d)** UV-Vis absorption spectrum of 600 μmol/L ascorbate solution and 200 μmol/L $CuSO_4$ solution when 20 μmol/L $HAuCl_4$ solution was added to the reaction mixture **(green curve)**.

As shown in Figure S5 and S6, when $HAuCl_4$ solution was mixed with ascorbate solution or together with Cu(II) at room temperature, the Au complex reduction by ascorbate would significantly hinder Cu(I) formation, which may retard the development of Alzheimer in Alzheimer-mice or its extension. When the $HAuCl_4$

solution was added to ascorbate solution at room temperature, the mixture immediately became a red turbid solution, indicating a rapid reaction rate. Meanwhile, when a regular amount of $HAuCl_4$ solution was gradually added to a mixture of 600 μmol/L ascorbate solution and 200 μmol/L $CuSO_4$ solution, the resulting mixture remained clear and thus the reaction could be readily monitored by UV-Vis spectrophotometry. The ultraviolet absorption spectroscopic study showed that the amount of Cu(I) from the reaction of ascorbate solution and $CuSO_4$ solution would be decreased substantially with continuously increase of the concentration of $HAuCl_4$ solution. This study suggests that it can be possible to utilize this new strategy to significantly decrease the generation of free radicals.

By comparing the Figure S6 **(a)** and Figure S5 **(B)**, it can be seen that the absorption peak at 314 nm of the new generated complex ascorbate-Cu(II) became stronger within 5 minutes, while there appeared another new absorption peak at 285 nm due to another complex ascorbate-Cu(I) formed from the redox reaction of ascorbate and $CuSO_4$ in aqueous solution. As shown in Figure S6 **(c, d)**, the absorption peak of ascorbate-Cu(I) almost disappeared and that of ascorbate-Cu(II) decreased substantially with continuous increase of the concentrations of $HAuCl_4$. It is obvious that gold nanoparticles apparently formed in the presence of ascorbate, as the relevant UV–Vis spectrum shows a broad band centered at about 550 nm, which is assigned to the plasmon band of Au nanoparticles (2–10 nm) [1, 2].

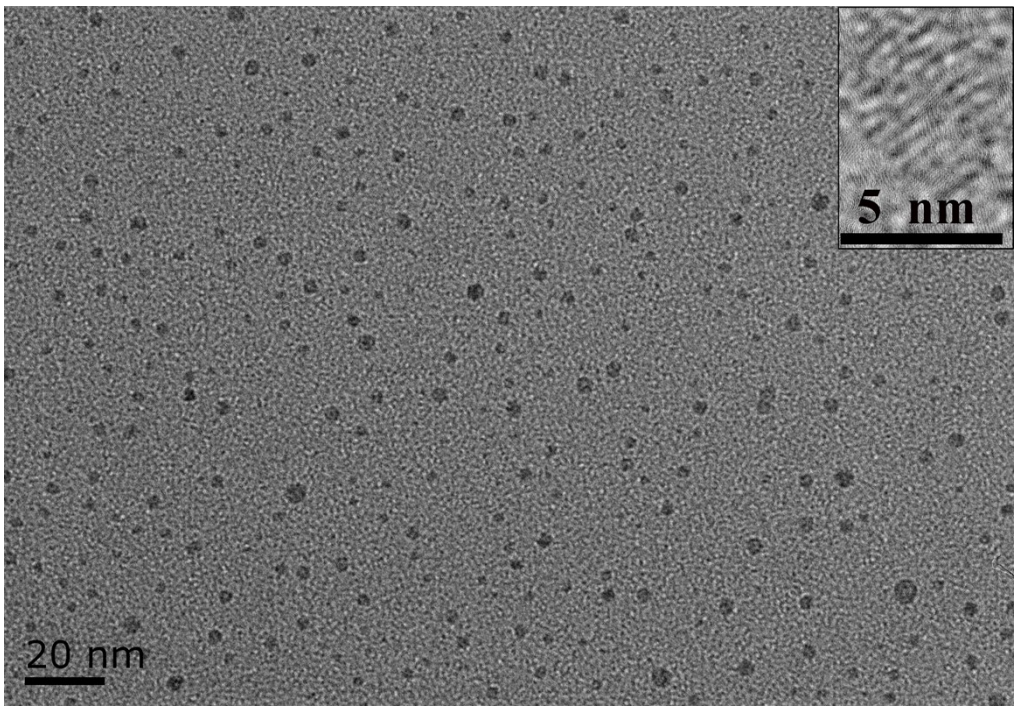

Figure S7 Typical TEM image of the generated Au NCs from the reaction of the mixture of 30 μmol/L ascorbate solution and 60 μmol/L $HAuCl_4$ solution, showing that the Au NCs are nearly spherical with no noticeable trend to aggregate. In Figure S7 (the inset), the HRTEM image indicates that the Au NCs kept their interplanar spacing of ~0.2 nm, which is basically identical to Au NCs from AD's brain and from the reaction of the mixture of 6 mmol/L $FeCl_2$ solution and 3 mmol/L $HAuCl_4$ solution.

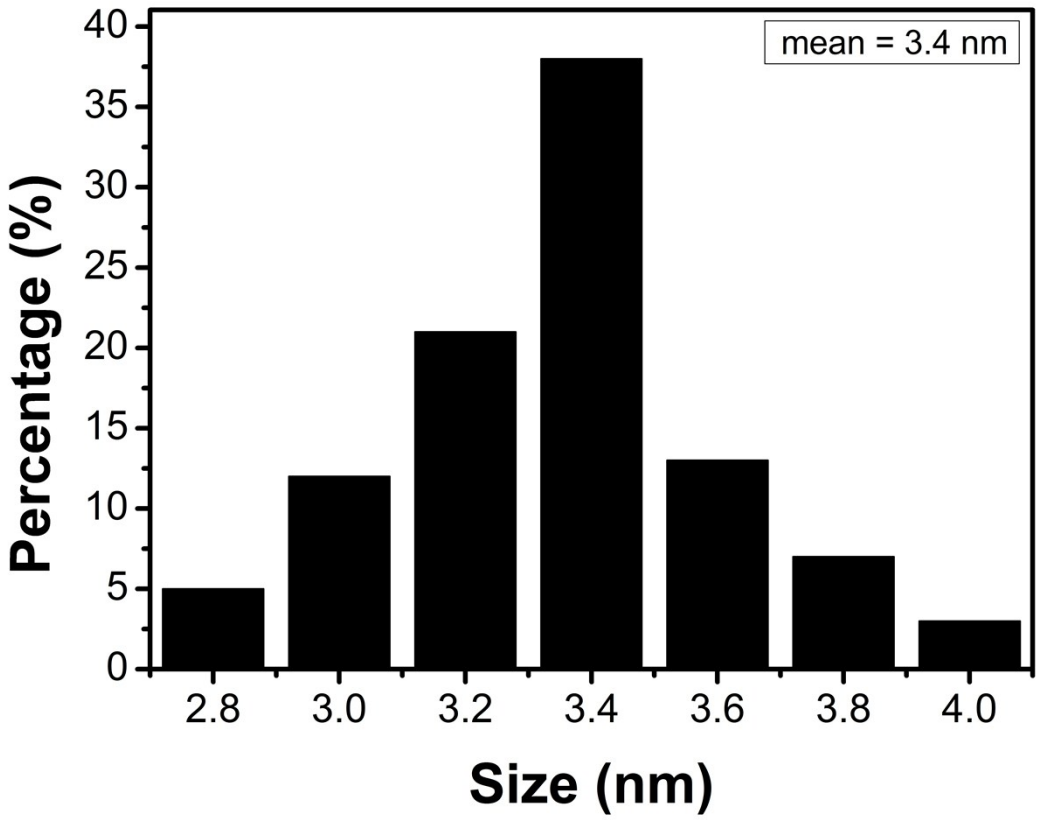

Figure S8 The size distribution of generated Au NCs in Figure S7 showing that 98% of the Au NCs ranged between 2.8 to 4.0 nm in diameter with a distribution peak at ca. 3.4 nm.

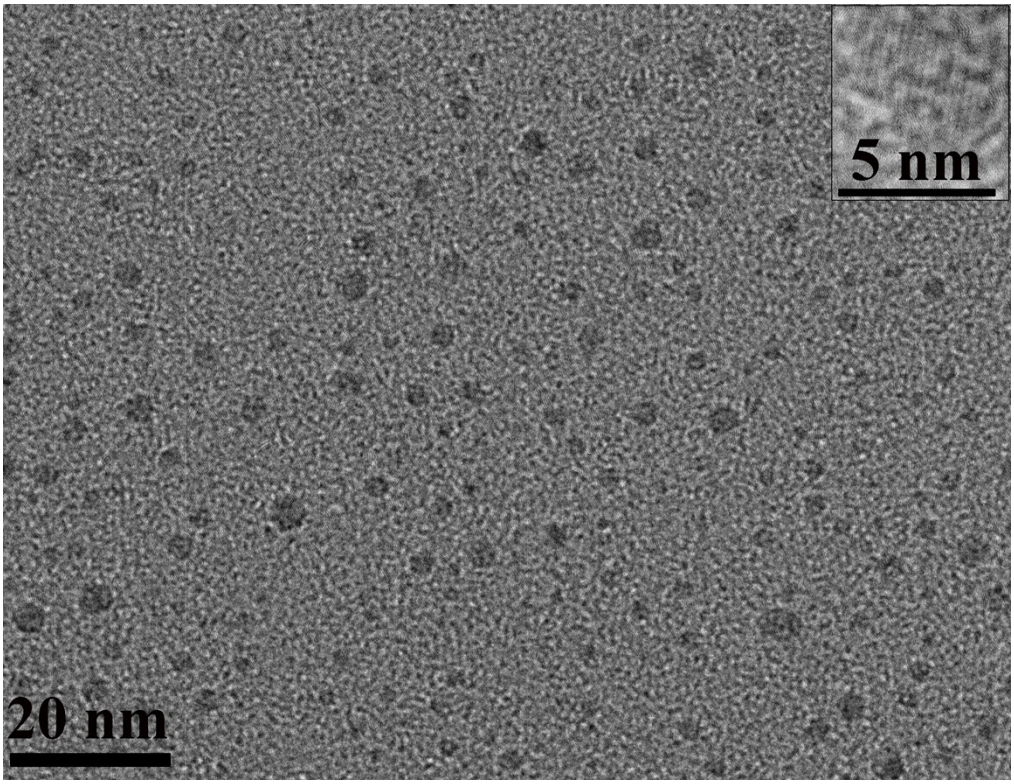

Figure S9 Typical TEM image of the resulting Au NCs from the reaction of the mixture of 6 mmol/L $FeCl_2$ solution and 3 mmol/L $HAuCl_4$ solution, showing that the Au nanoclusters are nearly spherical with no noticeable trend to aggregate. In Figure S9 (**the inset**), the HRTEM image indicates that the Au nanoclusters kept their interplanar spacing of ~0.2 nm, which is basically identical to Au nanoclusters from AD's brain.

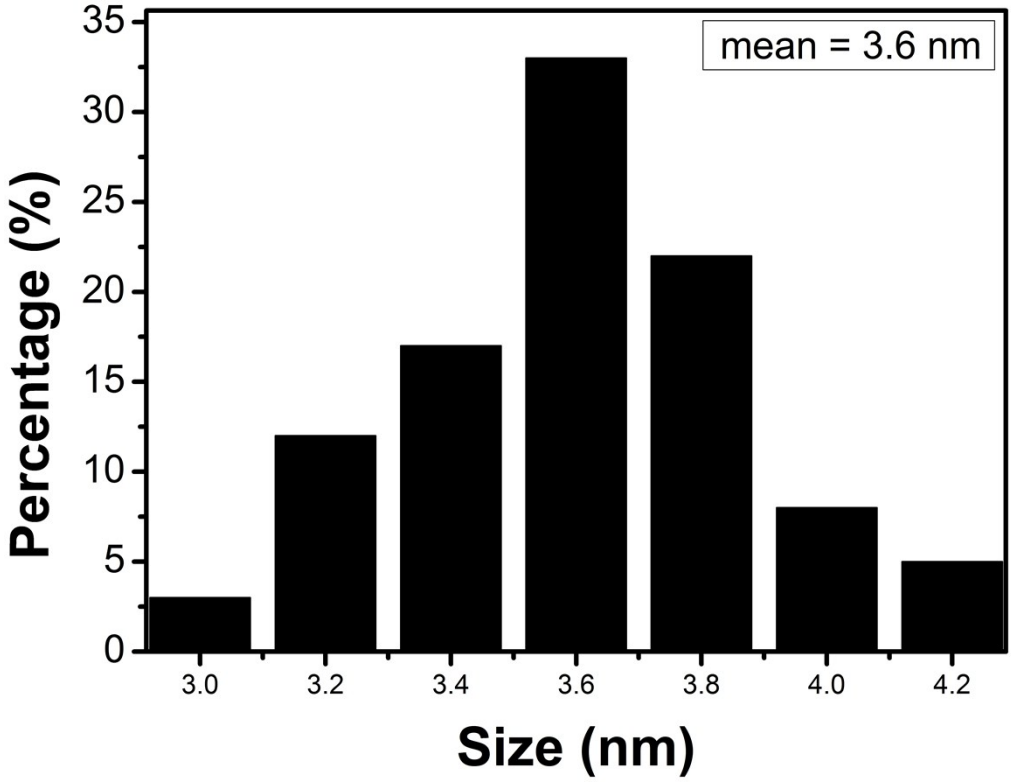

Figure S10 The size distribution of resulting Au NCs in **Figure S9** showing that 98% of the Au NCs ranged between 3.0 to 4.2 nm in diameter with a distribution peak at ca. 3.6 nm.

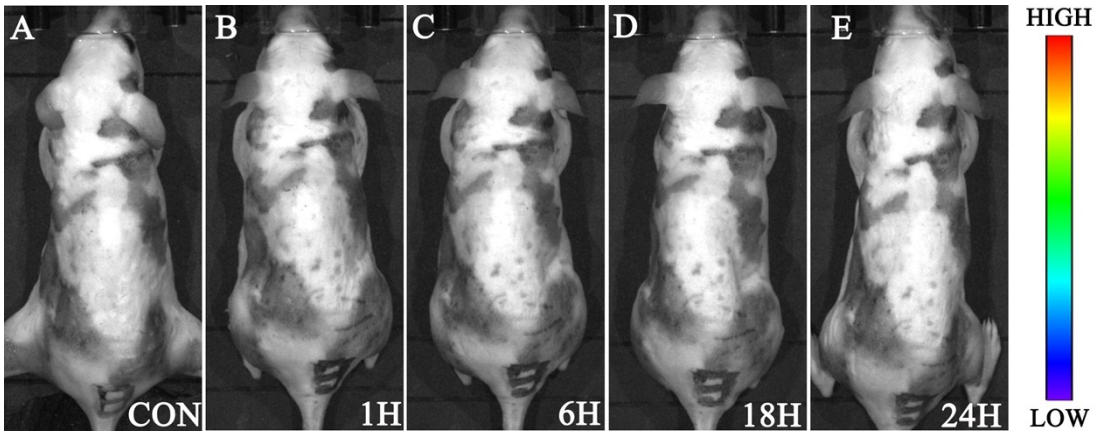

Figure S11 **A:** Fluorescence imaging of the blank normal control group of mice (**NOR**). **B-E:** Fluorescence imaging of the normal control group of mice at different time points via tail-vein injection of 10 mmol/L $HAuCl_4$ solution (1 H, 6 H, 18 H, 24 H). These control experiments demonstrated that there was almost no fluorescence in the normal control group of mice at different time points via tail-vein injection of $HAuCl_4$ solution.

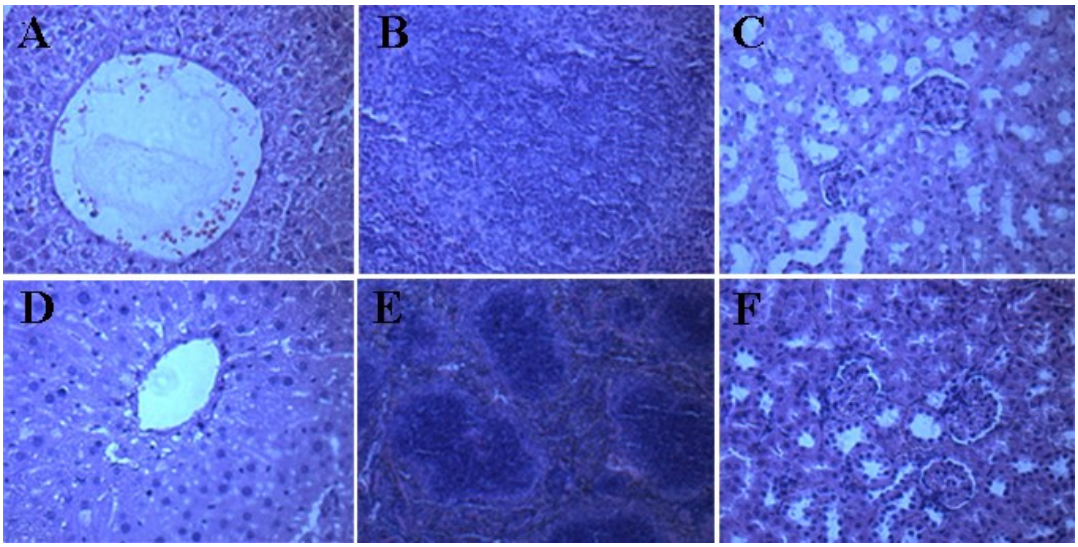

Figure S12 **(A, B, C)** Histopathologic analyses of H&E-stained tissue sections from the livers, spleens, and kidneys separately of blank normal group of mice without injection of $HAuCl_4$ solution. (**D, E, F**) Histopathologic analyses of H&E-stained tissue sections from the livers, spleens, and kidneys separately of blank control group of Alzheimer's model mice (**CON**) without injection of $HAuCl_4$ solution. Figure S12 (A-F) are magnified 40 times of objective. As seen in Figure S12, no appreciable pathological changes have been found in any of these organs of the blank normal group of mice and the CON.

Supplementary References

1 A. B. R. Mayer and J. E. Mark, *Eur. Polym. J.*, 1998, **34**, 103-108.

2 J. C. G. Martínez and R. M. Crooks, *J. Am. Chem. Soc.*, 2004, **126**, 16170-16178.